IEEE Access
Multidisciplinary | Rapid Review | Open Access Journal

Received October 2, 2020, accepted October 19, 2020, date of publication October 26, 2020, date of current version November 6, 2020.

Digital Object Identifier 10.1109/ACCESS.2020.3033852

Improving Passive Ankle Foot Orthosis System Using Estimated Ankle Velocity Reference

DIMAS ADIPUTRA[1], MOHD AZIZI ABDUL RAHMAN[2], (Senior Member, IEEE), UBAIDILLAH[3], (Senior Member, IEEE), AND SAIFUL AMRI MAZLAN[1]

[1]Electrical Engineering Department, Institut Teknologi Telkom Surabaya, Surabaya 60231, Indonesia
[2]Malaysia-Japan International Institute of Technology, Universiti Teknologi Malaysia, Kuala Lumpur 54100, Malaysia
[3]Mechanical Engineering Department, Universitas Sebelas Maret, Surakarta 57126, Indonesia

Corresponding author: Ubaidillah (ubaidillah_ft@staff.uns.ac.id)

This work was supported in part by the Ministry of Higher Education Malaysia under Grant 06G16, and in part by Universitas Sebelas Maret under Grant Hibah PKLP 2021.

ABSTRACT This study aims to investigate an appropriate ankle velocity reference (ω_{ref}), which is the average ankle velocity of a certain healthy subject when walking with a certain walking speed. The goal is to improve a Passive Controllable Ankle Foot Orthosis (PICAFO) by implementing the ankle velocity reference. Firstly, the function to estimate ω_{ref}, based on walking speed and body mass index (BMI), is obtained from 16 able-bodied subjects walking gait data. The effect of controlled stiffness (based on ω_{ref}) to the user's ankle kinematics and muscle activity was evaluated by comparing it to other settings, such as walking barefooted and various constant damping stiffness (0%, 30%, 60%, and 100% of the maximum damping stiffness). Two able-bodied subjects (normal and overweight) participated in the evaluation, where they had to walk at two different walking speeds (1 and 2 km/h). The result showed that ankle kinematics and muscle activity were improved when ω was controlled during walking speed of 1 km/h for both subjects. In terms of ankle kinematics, the toe clearance occurred, and walking stability increased. In terms of muscle activity, the average muscle activity had reduced by $\sim$29% for the normal subject and by $\sim$57% for an overweight subject, which shows that PICAFO provides necessary damping stiffness to replace the muscle works partially. In the future, by using the ω_{ref} based on walking speed and BMI, the therapists can skip the trial and error process of finding an appropriate PICAFO prescription for a post-stroke patient.

INDEX TERMS Ankle foot orthosis, ankle kinematic, ankle velocity, body mass index, damping stiffness, magnetorheological brake, muscle activity, passive control, walking gait, walking speed.

I. INTRODUCTION

A recently developed Ankle Foot Orthosis (AFO) by researchers had an articulated ankle joint with the addition of a mechanical actuator or electrical actuator to control the walking gait [1]. Researchers established control systems for automatic post-stroke rehabilitation using AFO. There are two approaches to controlling the AFO, such as active control and passive control. The actively controlled AFO can generate the walking posture [2], [3], and keeping the body balance [4], which is more suitable for amputee patients. Meanwhile, the passively controlled AFO controls the walking gait by restricting the foot movement to maintain the correct gait [5]. Despite the less functionality of passively controlled AFO compared to actively controlled AFO, patients with less gait impairment are suggested to have passively controlled AFO due to its simplicity and low cost.

A control reference is mandatory, which serves as a guide for the controller to control the gait properly. The control reference must suit the AFO user's needs to optimize the training benefits [6]. For instance, an active AFO tracks the predicted motion path, which suits the user's intention measured by EMG [7]. Another example is a passive AFO that maintains the correct walking gait by controlling the joint stiffness. Too much joint stiffness means high walking energy recruitment during push-off, but a slight joint stiffness means less gait assistance from the passive AFO is required [8].

The control reference is related to the mechanical properties of an AFO that can be controlled. In passive AFO, the mechanical properties, such as ankle velocity [9], [10],

The associate editor coordinating the review of this manuscript and approving it for publication was Jesus Felez.

and damping stiffness [11], [12] are controlled to maintain the correct walking gait. The adjustment of mechanical properties of passive AFO to suit the user's need can be accomplished before the usage using mechanical actuators (i.e., spring [13] and oil-damper [14]) or during the usage using electrical actuators, such as Magnetorheological (MR) devices (i.e., damper [15] and brake [16]). Damping stiffness is generated directly by the actuator. Meanwhile, the ankle velocity is controlled by applying appropriate damping stiffness. For instance, if the ankle velocity exceeds the reference, then the controller generates damping stiffness to reduce the ankle velocity.

Previous works had demonstrated damping stiffness control according to the gait phases [17]–[19]. For example, when the foot is on the ground, the stiffness is less generated, but the stiffness is more generated when the foot is in the air. However, there is no clear report on estimating the degree of damping stiffness to suits the user's needs. Instead, a trial and error attempt was executed to find the optimum damping stiffness [20]. The estimation of the damping stiffness reference is found to be challenging because it requires the Ground Reaction Force (GRF) information during walking performance [3], [21]. GRF is a force that resulted from the foot's contact on the ground. A multi-axis force transducer can be used to obtain the GRF information, but the sensor's bulky dimension may obstruct the AFO's sole surface.

Meanwhile, ankle velocity reference estimation is more practical than the damping stiffness reference estimation, which does not require the GRF information [22]. Kikuchi *et al.* [10] demonstrated an estimation of ankle velocity reference in the Initial Contact (IC) to the Foot Flat (FF) period only, which is associated with the users walking speed, such as slow, normal, and fast. Using the estimated ankle velocity reference, the passive AFO can adapt to different gait phases and different walking styles, such as the walking speed. Meanwhile, the subject's anthropometric, such as the Body Mass Index (BMI), has also been reported to contribute to a better estimation of ankle velocity reference, but it has yet to be implemented in a passive AFO system [22].

Therefore, there are two contributions to this study. The first contribution is to investigate ankle velocity reference function based on walking speed and BMI in four distinct gait phases [22]. Phase 1 is from IC to FF, Phase 2 is from FF to Heel Off (HO), Phase 3 is from HO to Toe Off (TO), and Phase 4 is the swing phase. The second contribution is to improve a passive AFO equipped with an MR brake, called PICAFO (Passive Controllable AFO), by implementing the ankle velocity reference. By doing so, the previous version of PICAFO [16] can be improved in terms of appropriate control reference that can be straightforwardly estimated. Because of this, the PICAFO's user is expected to get benefits using the PICAFO for walking, such as better ankle kinematics with less muscle activity [8] and less energy [3].

Section II describes the PICAFO system. Section III discusses the estimation of the ankle velocity reference based on the walking speed and BMI. Statistic parameters are used to observe the strength of including BMI as the estimator instead of the walking speed only. Section IV presents the implementation of the ankle velocity reference on the PICAFO system. Implementation results are also discussed in terms of ankle kinematics and muscle activity when the user walks using PICAFO with the ankle velocity reference compared to several constant damping stiffness references, such as zero (0%), low (30%), medium (60%, and high (100%) damping stiffness. Lastly, Section V concludes the study.

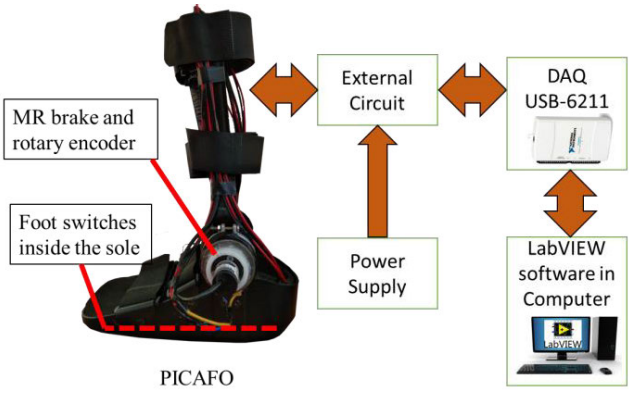

FIGURE 1. The overall architecture of PICAFO prototype.

For your information, the orthopedic doctor's committee, Institutional Review Board of Education Hospital of Universitas Sebelas Maret, Indonesia, in an approval letter no. 893/UN27.49/TU/2018 declared that the walking experiment in this study is safe for the category of work involving human subjects. The subjects also gave their written consent before the experiment was executed.

II. PASSIVE CONTROLLABLE AFO (PICAFO)

A. PICAFO TEST RIG

Overall, PICAFO's architecture is shown in Fig. 1. The prototype structure was made by modifying a commercial Air Ankle Boot produced by China OEM, which initially had an articulated ankle joint and adjustable ankle ROM (maximum -45 to 45 degree). An MR brake at the ankle joint generates controllable damping stiffness [23], [24]. The MR brake is a T-shape brake [25], where the gap is filled with MR fluid LORD-132DG. The MR brake is powered using an external power supply. At 0% damping stiffness state or when the current is equal to zero, the damping stiffness is 0.34 Nm. Meanwhile, the 100% damping stiffness is 2.05 Nm when the maximum current of 1 A is applied.

There are rotary encoders at the ankle joint and footswitches inside the foot insole as the sensing unit. The rotary encoder returns a positive ankle position for dorsiflexion and a negative ankle position for plantarflexion. The zero radiant ankle position is the rotary encoder's ankle angle position when the subject stands up still (neutral position). The footswitches are located on the heel and toe to classify the walking gait into 4 phases. The gait phases are P1: Initial Contact (IC) to Foot Flat (FF), P2: FF to Heel Off (HO),

TABLE 1. List of regression analysis cases.

Case	Phase	BMI	WS
1		√	
2	IC TO FF (P1)		√
3		√	√
4		√	
5	FF TO HO (P2)		√
6		√	√
7		√	
8	HO TO TO (P3)		√
9		√	√

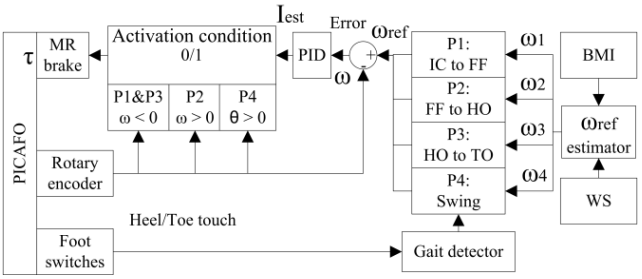

FIGURE 2. PICAFO controller.

P3: HO to Toe Off (TO), and P4: swing. For data monitoring and logging, all the sensors and actuators are connected to LabVIEW on the computer through a USB-6211 Data Acquisition from National Instrument. An external circuit is available to bridge the electronic components.

B. CONTROLLER

In general, the PICAFO prototype controls the walking gait based on the ankle velocity reference (ω_{ref}), which is estimated based on walking speed and BMI, as shown in Fig. 2. There are four ankle velocity references (ω_1, ω_2, ω_3, ω_4) for each of the four gait phases (P1 – P4) detected by the footswitches. The PID controller controls the ankle velocity (ω) according to ω_{ref} by calculating I_{est} for the MR brake to generate appropriate stiffness. If the ankle velocity exceeds the control reference in the same direction, then the MR brake would apply appropriate stiffness to reduce the ankle velocity. On the other hand, the MR brake will do nothing if the activation condition is not fulfilled. The activation condition of P1 and P3 is when ω is less than zero. When ω is more than zero, the activation condition of P2 is fulfilled. Meanwhile, the activation condition during P4 is when θ is more than zero.

III. ANKLE VELOCITY REFERENCE ESTIMATION

A. DATA COLLECTION

The purpose of controlling the ankle velocity using PICAFO is to maintain the correct walking gait; in other words, a healthy walking gait. Therefore, ω_{ref} estimation function was established by utilizing ω data of able-bodied subjects with different BMI walking at different walking speeds. A total of 16 young (24 – 29 years old) male able-bodied subjects who participated in the walking experiment (n = 16) participated in this study. The subject's BMI varied in 3 categories: underweight (n = 4), normal (n = 6), overweight (n = 6). The subject was required to walk on a treadmill with constant walking speed and variations of 1, 3, and 5 Km/h, which represented slow, decent, and fast walking speed. The walking gait data was measured using lower limb plug-in gait in the VICON motion capture system [26]. Each step data consisted of approximately 60 to 260 data points, depending on the step period (sampling frequency was 100 Hz). In one session, there were 30 steps of captured walking data being selected for further processing. There was a total of 48 sessions (16 subjects x 3 walking speed). Therefore, there were 1440 sets of walking data that were used for establishing ω_{ref} estimation function.

B. DATA PROCESSING

The measured walking gait data involved in the ankle position. The difference between the initial ankle position and the final ankle position in one phase was divided by the time-lapse, which defined the average ω, as presented in previous work [10], [22]. Further analysis involved regression analysis with statistic parameters, such as R-value, standard of error, and t-test. As mentioned earlier, the previous work by Kikuchi *et al.* [10], [27] only showed ankle velocity reference estimation based on the walking speed. The statistic parameters of 9 different cases were compared to observe BMI's strength as an additional estimator in ω_{ref} function, as shown in Table 1. The ω_{ref} estimation was investigated for P1 until P3. Meanwhile, on P4, the ω_{ref} estimation was not investigated. The PICAFO could straightforwardly apply maximum stiffness to lock the ankle joint ($\omega = 0$), which ensured toe clearance on P4 regardless of the subject's walking speed and BMI [17], [28], [29].

There are two critical parameters to build ω_{ref} function, such as the walking speed X1 and BMI X2. The statistic parameters of the regression analysis explain the relationship between the critical parameter and control reference. The R-value

$$R = \sqrt{1 - \left(\frac{\sum_{i=1}^{n} E_i^2}{\sum_{i=1}^{n} (\omega_i - \omega_{mean})^2} \right)} \quad (1)$$

describes the correlation score of critical parameters to the ankle velocity, where n is the sample-numbers, E_i is the residual between the estimated ω_{ref} and the actual ω, ω_i is the i-th actual ω data, and ω_{mean} is the average ω. The absolute R-value showed the correlation. If the R-value is positive, it means a positive correlation, and if the R-value is negative, then it means a negative correlation. The absolute R-value that approaches one means a better correlation. Meanwhile, the standard of error (Se)

$$Se = \sqrt{\frac{\sum_{i=1}^{n} E_i^2}{(n-1)}} \quad (2)$$

TABLE 2. Regression statistics result.

Phase	Regression statistics	X1 estimation	X2 estimation	X1&X2 estimation
(P1)	R-value	-0.21	-0.201	-0.292
	Standard Error	24.212	24.263	23.692
(P2)	R-value	0.702	0.115	0.712
	Standard Error	13.056	18.207	12.868
(P3)	R-value	-0.711	-0.223	-0.747
	Standard Error	35.265	48.868	33.336
	Observations	1440	1440	1440

indicated the nature of the relationship, where a lesser standard of error indicates a better relationship. The ω_{ref} function was build based on the linear equation of walking speed and BMI samples data. Given the covariance of two samples s_1 and s_2

$$cov(s_1, s_2) = \frac{\sum_{i=1}^{n}(s_{1_i} = \bar{s_1})(s_{2_i} - \bar{s_2})}{n-1} \tag{3}$$

the walking speed coefficients (b_1) and BMI coefficient (b_2) of ω_{ref} function are obtained by solving

$$\begin{aligned} cov(\omega, \text{X1}) &= b_1 cov(\text{X1}, \text{X1}) + b_2 cov(X2, X1) \\ cov(\omega, \text{X2}) &= b_1 cov(\text{X1}, \text{X2}) + b_2 cov(X2, X2) \end{aligned} \tag{4}$$

Then, the probability of the critical parameter coefficients, b_1 and $b_{2,}$ being zero is explained by performing a t-test

$$t = \frac{b_j}{s\sqrt{c_{jj}}} \tag{5}$$

where b_j is critical parameter coefficients (j = 1, 2), c_{jj} is variances of b_j, and s is the residual (E_i) mean square. Based on the t statistics, the p-value can be found. If the coefficient is zero (p-value > 0.05), then it means that the critical parameter is insignificant for estimating the control reference.

C. RESULT OF ANKLE VELOCITY REFERENCE ESTIMATION

The correlation of critical parameters (X1, X2, and X1&X2) with ω is negative during P1 and P3, while the correlation is positive during P2, as shown by R-value in Table 2. A negative correlation means that the higher the critical parameter, the higher the ankle velocity in the negative direction (plantarflexion), and a positive correlation means the opposite (dorsiflexion). Here, the foot movement is plantarflexion in P1 and P3, and dorsiflexion in P2. For an illustration of the regression analysis result, readers can refer to Appendix A. The estimation based on X1&X2 produces the highest correlation score for all phases. The standard error result also agrees, where X1&X2 estimation produces the least standard error compared to other estimation.

Meanwhile, Table 3 shows the critical parameter coefficient analysis. Both b_1 and b_2 have a similar coefficient sign, as shown in Table 3. The walking speed is the more significant critical parameter than BMI, as reflected by a higher b1 compared to b_2. Despite the less significant of b_2 than b_1, the probability of the b_2 to be zero is very unlikely,

TABLE 3. Critical parameter coefficient result analysis.

P1	Coefficients	t-Stat	p-value
c	0.36	0.01	0.924
b_1	-3.24	-8.37	< 0.05
b_2	-1.22	-7.99	< 0.05
P2	Coefficients	t-Stat	p-value
c	-7.15	-3.54	< 0.05
b_1	7.93	37.67	< 0.05
b_2	0.54	6.54	< 0.05
P3	Coefficients	t-Stat	p-value
c	36.92	7.06	< 0.05
b_1	-21.96	-40.33	< 0.05
b_2	-2.79	-13.02	< 0.05

as shown by the p-value < 0.05. The only thing that might be zero is the intercept c, of estimation on P1 (p-value = 0.924), which does not affect the contribution of the critical parameters to ω_{ref} estimation in general.

In summary, the result implies that the addition of BMI improves ω_{ref} estimation. Compared to a previous study conducted by Kikuchi *et al.* [10], where the ankle velocity has a clear proportional relationship with walking speed, the relationship between ankle velocity and BMI needs further explanation. The total torque around the ankle joint affects the joint's angular acceleration [30]. The higher the ankle torque, the higher the angular acceleration, which also means higher ankle velocity. Several forces contribute to the total torque around the ankle joint during walking, such as ankle force, foot weight, and GRF. The body mass affects the force amount, as observed in higher BMI persons with higher GRF [31], [32]. The foot torque's length depends on the foot length. A taller person is most likely to have a longer foot length compared to a shorter person. Thus, a taller person is most likely to have a higher ankle torque [33]. Other research also reports that a higher BMI person has shorter strides [34]; thus, if that person walks at the same walking speed as another person with lower BMI, the shorter stride length will result in higher ankle velocity. Compromise all this information leads to the possibility of a relationship between ankle velocity and BMI. The regression analysis result has confirmed that ω_{ref} has a proportional relationship with walking speed and BMI, fulfilling the first contribution. Table 4 shows the ω_{ref} function

$$\omega_{\text{ref}} = (\text{c} + \text{b}_1\text{X1} + \text{b}_2\text{X2}) \times 0.017453\,\text{rad/s} \tag{6}$$

for the PICAFO system in radians unit, where c, b_1, and b_2 are obtained from Table 3. Therefore, each phase has a different ω_{ref} estimation. The ω_{ref} estimation of P1 – P3 can be done by merely inserting the desired walking speed X1 (i.e., treadmill speed during training) and the subject's BMI X2 to the ω_{ref} estimation function. Meanwhile, the ω_{ref} of P4 is equal to zero without considering the critical parameters because locking the ankle position for toe clearance during P4 can be done by putting maximum damping stiffness, regardless of the walking speed and BMI [11], [16]. The derived ω_{ref} function

TABLE 4. PICAFO controller reference.

Phase	Activation condition	ω_{ref} estimation function (rad)
(P1)	Plantarflexion ($\omega < 0$)	$\omega_{ref} = 0.0063 - 0.057$ WS $- 0.021$ BMI
(P2)	Dorsiflexion ($\omega > 0$)	$\omega_{ref} = -0.125 + 0.138$ WS $+ 0.009$ BMI
(P3)	Plantarflexion ($\omega < 0$)	$\omega_{ref} = 0.644 - 0.383$ WS $- 0.049$ BMI
(P4)	Positive ankle position ($\theta > 0$)	$\omega_{ref} = 0$

only represents a small population of samples (n = 16). Thus, the implementation of this control reference was focused on the small population in this research first. The purpose is to demonstrate the strength of estimating the control reference rather than trial and error to find the appropriate damping stiffness. Afterward, the ω_{ref} function should be improved by inviting a large sample population for more generalization. The pre-clinical evaluation can also be considered by creating a machine that simulates the variables' incremental variation and wears the PICAFO system to the extreme.

IV. IMPLEMENTATION OF THE ANKLE VELOCITY REFERENCE

The implementation has been conducted to achieve the second contribution of this research, improving the previous version of PICAFO by implementing the ankle velocity reference. It is expected that the users can benefit when using PICAFO with the controlled stiffness based on the ω_{ref}, in terms of ankle kinematics and muscle activity.

A. DATA COLLECTION

Two subjects from the previous 16 subjects were invited back for the implementation of ω_{ref} using the PICAFO system. Subject 1 (S1) has a normal BMI of 22.2, while Subject 2 (S2) has an overweight BMI of 28.7. The subjects also had to walk on a treadmill with constant walking speed, WS1 (1 km/h), and WS2 (2 km/h), and different joint stiffness conditions instead of being barefooted. Walking speed of 1 and 2 km/h was chosen to replicate post-stroke condition who cannot perform fast walking [35], [36] whom PICAFO is intended for. There are 6 PICAFO stiffness conditions, which are zero stiffness, low stiffness (30%), medium stiffness (60%), high stiffness (100%), and controlled stiffness (the damping stiffness is based on ω_{ref} estimation in Table 4). There are four cases (2 BMI x 2 walking speed) and six stiffness conditions. Therefore, there are a total of 24 data collection sessions, where 30 walking gait data are selected in each session.

The walking gait data are ankle kinematics and muscle activity. The ankle kinematics data, during PICAFO assistance, such as ankle position (θ) and ankle velocity (ω), were collected using a rotary encoder in the PICAFO prototype. Meanwhile, the ankle kinematics data taken during barefooted walking were collected using the VICON motion capture system. As for the muscle activity, the RMS electromyography (EMG) of Tibialis Anterior (TA) and Gastrocnemius (G) muscles were collected using a Biopac instrument and Acqknowledge software. Firstly, the raw EMG data were gathered with a sampling frequency of 1000 Hz [37]–[40]. Then, the raw EMG is filtered using a low pass filtered (cut-off frequency of 6 Hz) and rectified before the RMS EMG is calculated [8].

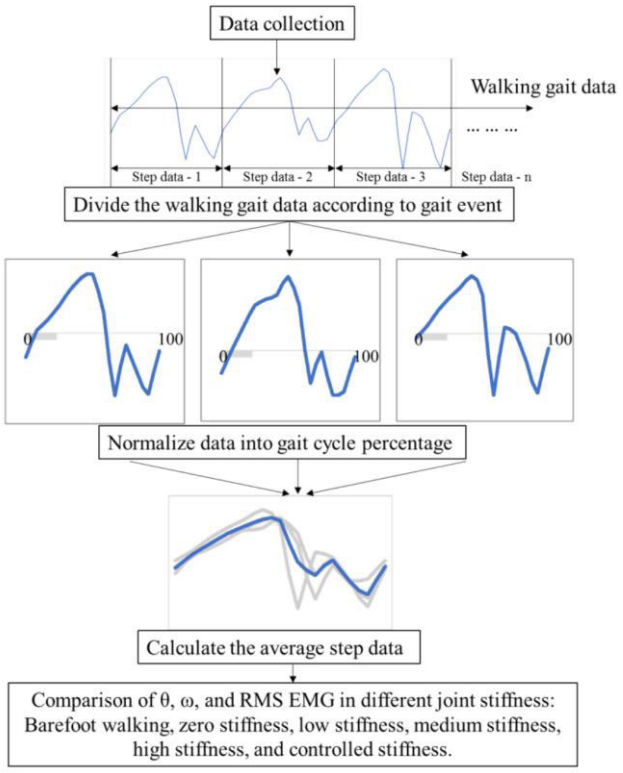

FIGURE 3. Overview of walking gait data processing.

B. DATA PROCESSING AND ANALYSIS

Fig. 3 displays an overview of the data processing. First, the walking gait data (θ, ω, and RMS EMG) are divided using the gait events. These divided data are called step data. The step data began from the IC, which ended on the next IC of the same leg. Next, the data is normalized based on the gait completion or gait cycle percentage. IC is 0%, and the next IC is 100% of the gait cycle. After normalizing the time domain data to the gait cycle percentage data, the average of step data in one case is calculated by averaging the data point of the step data to build a whole average step data.

Data analysis is accomplished by comparing the average steps of data according to different joint stiffness. For θ comparison, the ankle Range of Motion (ROM), ankle push-off, and toe clearance are the observation highlights, as shown in Fig. 4. Meanwhile, the ω is compared with ω_{ref} to see the effect of applying different ankle joints' stiffness. For statistics comparison, the variances of θ and ω describe the walking stability. Lower variance means a more stable

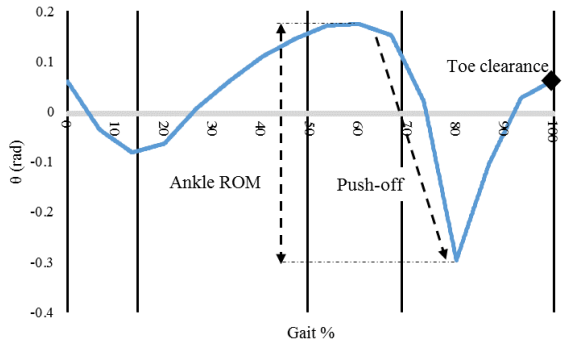

FIGURE 4. Definition of ankle ROM, push-off, and toe clearance.

walking gait parameter [41]. The t-test was also performed to see the significance of the PICAFO stiffness compared to barefooted walking and zero stiffness.

The average step data of RMS EMG compare the muscle activity between different PICAFO joint stiffness for each case. The average muscle activity (AMA) in one gait cycle

$$\text{AMA} = \frac{\int_0^{100} NRE\, d\%}{100} \tag{7}$$

of the TA and G compares the muscle activity between different PICAFO joint stiffness for each case, where NRE is the normalized RMS EMG, and % is the gait percentage. The RMS EMG data were normalized first to the maximum average RMS EMG of walking barefooted in one case for comparison purposes. The RMS EMG is normalized per case because the MA of walking barefooted is different for each case [8].

Replacing the muscle's work using an actuator that works in unison will decrease the muscle activity [42], [43]. TA works in dorsiflexion, where it keeps ω during P1 [44], and ensures toe clearance during P4 [37]. Meanwhile, G is responsible for plantarflexion, where it maintains the forward force during P2 to avoid over-extending [45]. In this case, the reduction of TA and G muscle activity is expected when assisted by the MR brake with appropriate stiffness because it has the same working principle, which restricts the foot movement.

C. ANKLE KINEMATICS RESULT

Fig. 5 shows the average ankle kinematics in the different ankle joint stiffness for case S1-WS1. Please refer to Appendix B for ankle kinematics results of other cases. Walking with a variable stiffness of PICAFO significantly affects the ankle's ROM, push-off ability, and toe clearance compared to walking barefoot and walking with zero stiffness PICAFO (p-value $<$ 0.05). Refer to Fig. 5 (a), the ankle ROM (1) is more restricted upon using PICAFO. However, the higher the stiffness does not necessarily be felt in the lowest ankle ROM. On P1, the angular distance between the lowest ankle position and initial ankle position (2) and duration to reach it (3) are affected by ankle joint stiffness.

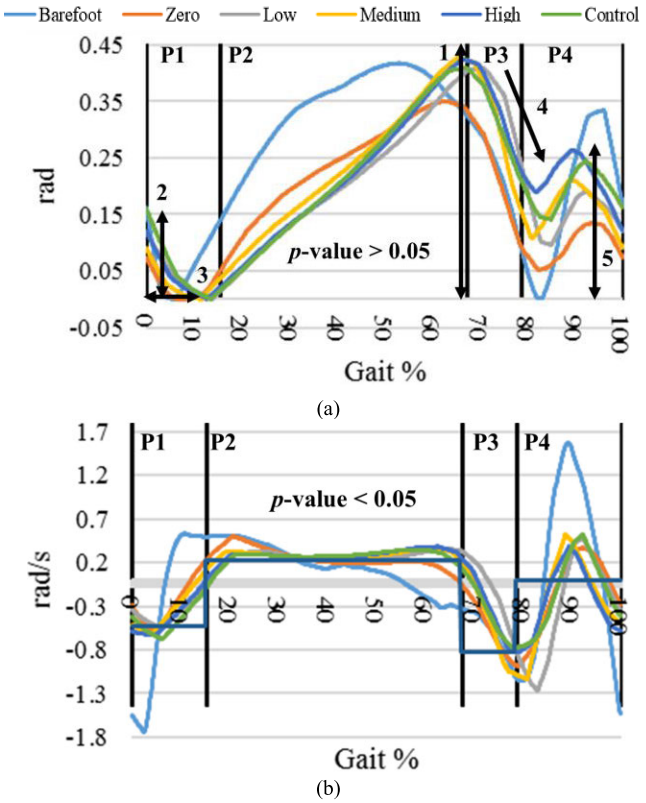

FIGURE 5. Average ankle kinematics in different joint stiffness for case S1-WS1: (a) ankle position; (b) ankle velocity (ω_{ref} shown in solid straight line).

The angular distance on P1 during barefooted walking is longer, and the duration to reach the lowest ankle position is shorter compare to walking with PICAFO. When the subject walks using PICAFO, the ankle angular distance becomes smaller, but the duration is longer.

Meanwhile, the toe clearance (4) from P3 to the mid of P4 still appears in all the cases. Toe clearance appearance is natural since the subjects are healthy. However, the able-bodied subjects do not require much ankle position recovery after the push-off when walking with the assistance of PICAFO (5), which can be seen from the ankle position that does not drop much. The PICAFO maintains the ankle position by retaining the ankle position above the neutral position, ensuring clearance without ankle position recovery.

Although the ankle position is significantly different due to different ankle joint stiffness, the ankle velocity, ω, does not change much before and after the use of PICAFO with different stiffness (p-value $>$ 0.05). The similarity is especially apparent for P2 and P3, but not for P1 and P4 because the foot moves when walking barefooted. Refer to Fig. 5 (b), ω approaches the ω ref (shown in a straight line) better when the stiffness is controlled. For example, at the end of P3, the ω of zero, low, and medium stiffness exceeds the ω ref, but ω resulted from controlled and high stiffness does not exceed ω ref. This result indicates that the use of PICAFO with controlled and high stiffness can help maintain the ankle

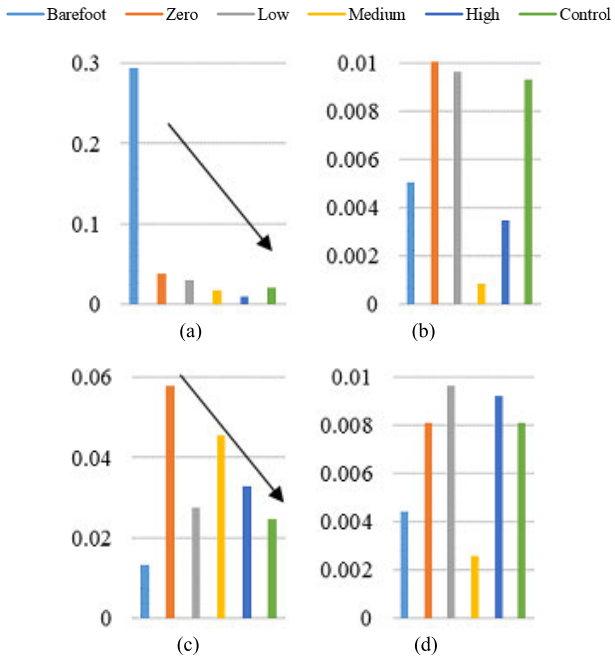

FIGURE 6. Step period variance in different joint stiffness: (a) S1-WS1, (b) S1-WS2, (c) S2-WS1, (d) S2-WS2.

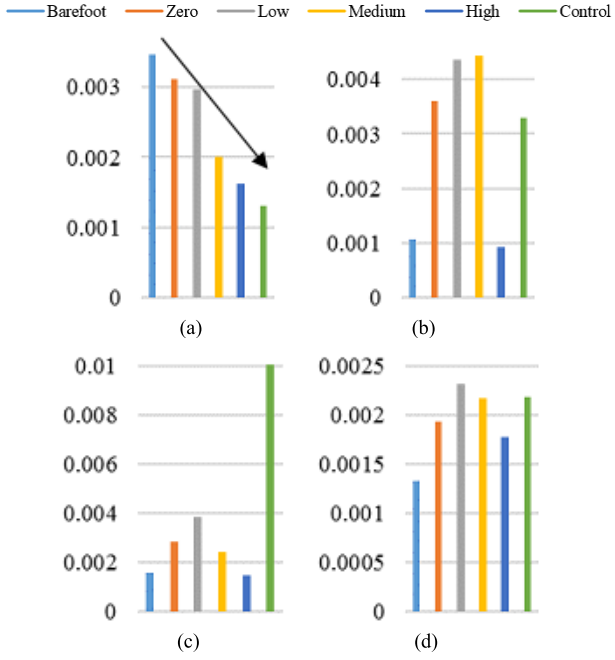

FIGURE 7. Ankle position variance in different joint stiffness: (a) S1-WS1, (b) S1-WS2, (c) S2-WS1, (d) S2-WS2.

velocity in S1-WS1's case. However, the control stiffness consumes less energy in terms of energy efficiency because the MR brake only generates the stiffness when necessary.

Meanwhile, in S2 (see Appendix B), the ω never approaches the reference during P1, P2, and P3, except during P4, where the controller controls the ω to reach 0 rad/s. Even when walking barefooted, the ω also does not approach ω_{ref}

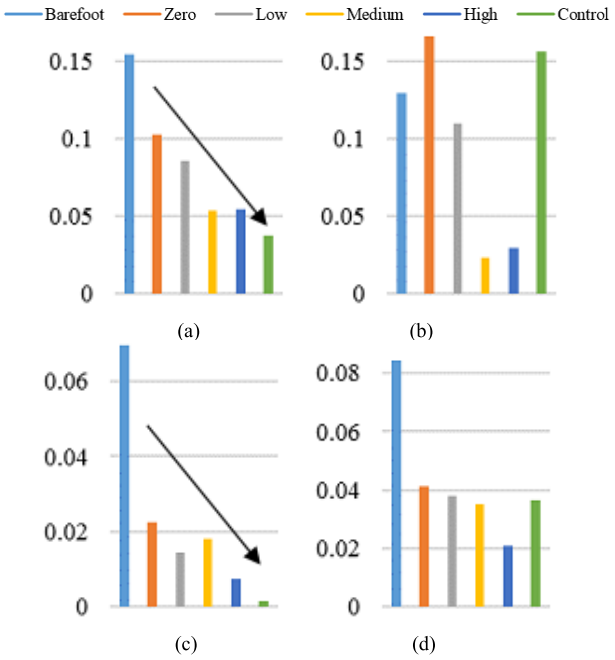

FIGURE 8. Ankle velocity variance in different joint stiffness: (a) S1-WS1, (b) S1-WS2, (c) S2-WS1, (d) S2-WS2.

despite the functions derived from ankle velocity data of healthy subjects that walked barefooted. This result shows that the ω_{ref} function is more accurate for S1 compared to S2 to estimate the control reference. In this scenario, the PICAFO will not make any attempt to correct the ankle velocity since it never exceeds the ω_{ref}. Improvement of the estimation should be done in future work, such as by increasing the sample sizes.

Fig. 6, 7, and 8 show the variance of step period, ankle position, and ankle velocity, respectively, in all cases as an effect of different joint stiffness. All the variances are small in general (less than 0.05), which demonstrates PICAFO reliability for collecting the data. The variance value varies due to different joint stiffness. When the subject walked with zero stiffness PICAFO, the ankle position variance, and step period increase, while the variance of ankle velocity decreases. If joint stiffness is applied, then all the variance is smaller compare to variance resulted from zero stiffness. Using the controlled stiffness resulted in the lowest variance of gait parameters. The result is similar across the two subjects but not similar to different walking speeds. In the WS1 case (a and c in Fig. 6, 7, and 8), the lowest gait parameter variance occurs due to applied control stiffness. However, in the WS2 case (b and d in Fig. 6, 7, and 8), the control stiffness is inferior in maintaining the gait variance, while high stiffness is more superior.

Controlling the gait in faster walking speed requires more stiffness because the ankle torque is higher, which explains the superiority of the constant high stiffness compared to the controlled stiffness in the case of WS2. The MR brake capacity should be improved to cope with this situation.

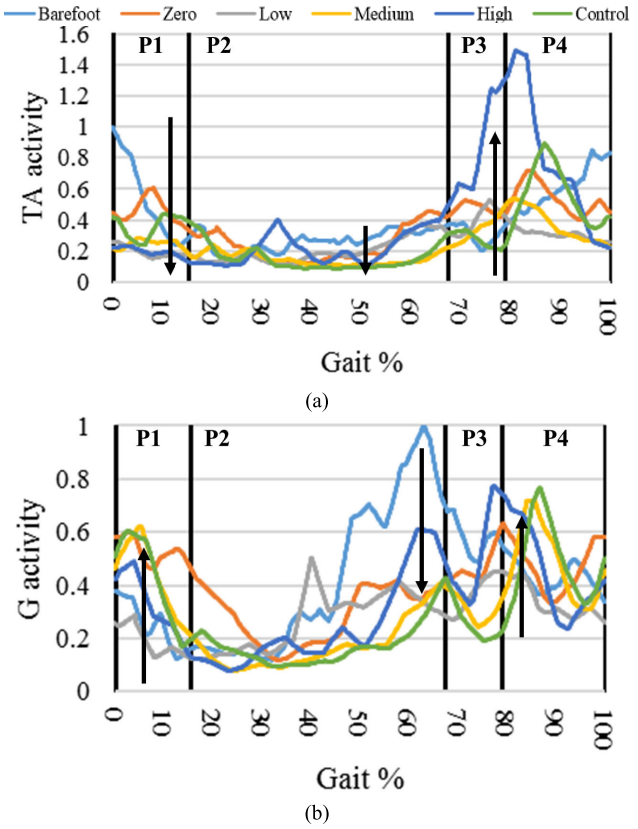

FIGURE 9. RMS EMG of muscle activity in different joint stiffness for case S1-WS1: (a) Tibialis Anterior activity; (b) Gastrocnemius activity.

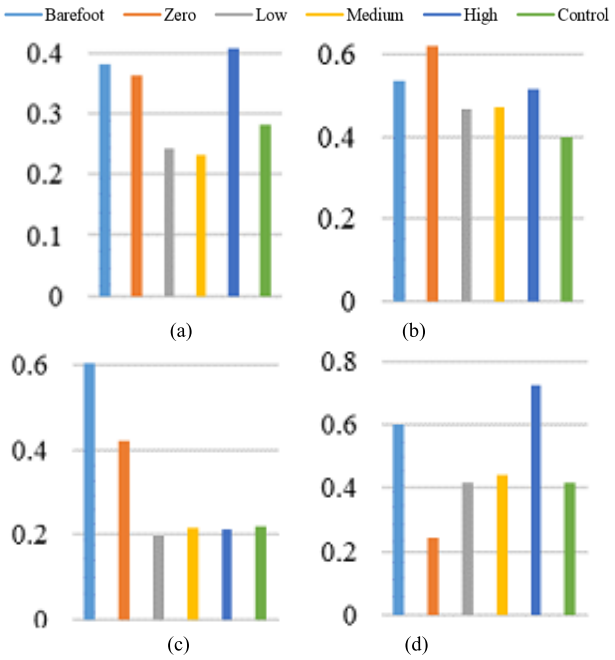

FIGURE 10. Average TA activity in different joint stiffness: (a) S1-WS1, (b) S1-WS2, (c) S2-WS1, (d) S2-WS2.

However, in rehabilitation, the post-stroke patient usually ambles (walking speed $\leq$ 2 Km/h) [35], [36]. Thus, it is suitable for him/her to be assisted using the PICAFO in this study. Therefore, the modification on the MR brake capacity is only necessary if the PICAFO is used outside of rehabilitation.

D. MUSCLE ACTIVITY RESULT

PICAFO decreases the walking muscle activity in P1 and P2 but not in P3 and P4, as shown in the case sample S1-WS1 in Fig. 9. Please refer to Appendix C to see the muscle activity result of the other case.

In P1, when the subjects use the PICAFO, the TA activity decreases, but the G activity gets higher instead (except for S2-WS2's case where both TA and G activities decrease). At this phase, the main movement is plantarflexion as the foot moves to reach the foot flat from the initial contact position. The G generates the movement, while TA provides braking torque at the same time. As a result of using PICAFO, the G activity increases because the PICAFO restricts the plantarflexion. In contrast, the TA activity decreases because the PICAFO joint stiffness replaces the work. However, more stiffness does not always mean more G increment or TA reduction for both subjects. For the S1-WS1 case, the lowest TA activity occurs when the stiffness is high. Nevertheless, in the case of S2-WS1, the lowest TA activity belongs to PICAFO with controlled stiffness.

TABLE 5. Muscle activity reduction due to PICAFO assistance compare to walking barefooted.

Case	Ankle stiffness	TA activity	G activity	Overall muscle activity
S1-WS1	Zero	-5%	-8%	-6%
	Low	-36%	-32%	-33%
	Medium	-39%	-30%	-34%
	High	+7%	-21%	-8%
	Control	-26%	-31%	-29%
S1-WS2	Zero	+16%	+11%	+13%
	Low	-12%	+5%	-3%
	Medium	-12%	+20%	+6%
	High	-4%	+38%	+20%
	Control	-25%	+71%	+29%
S2-WS1	Zero	-30%	-21%	-26%
	Low	-67%	-51%	-60%
	Medium	-64%	-54%	-60%
	High	-65%	-58%	-62%
	Control	-63%	-48%	-57%
S2-WS2	Zero	-60%	-57%	-58%
	Low	-31%	-59%	-46%
	Medium	-26%	-52%	-41%
	High	+21%	-35%	-11%
	Control	-30%	-26%	-28%

On P2, the TA and G activities decrease with a significant reduction in the G activity, and the result is similar for all cases involving the subjects and the walking speed. In this phase, the main ankle movement is dorsiflexion, with the body weight shifted to the direction of walking. The TA muscle activity, which is responsible for dorsiflexion, can be seen in the barefoot walking data for case S1-WS2 and S2-WS1.

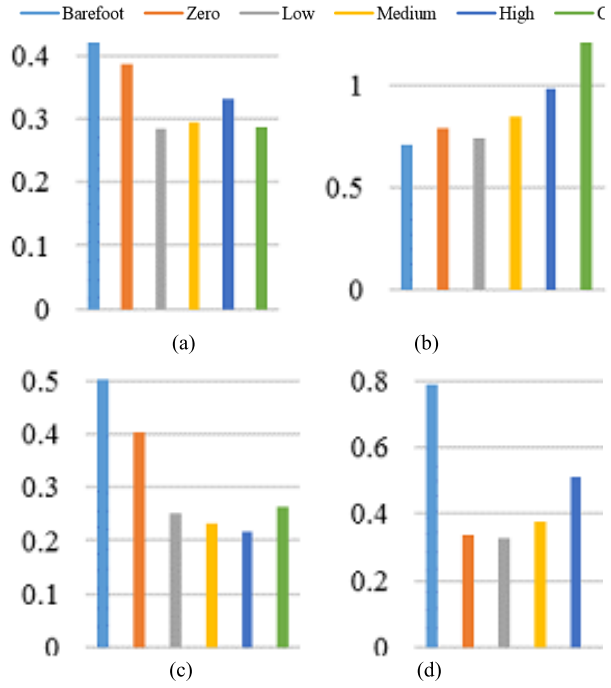

FIGURE 11. Average G activity in different joint stiffness: (a) S1-WS1, (b) S1-WS2, (c) S2-WS1, (d) S2-WS2.

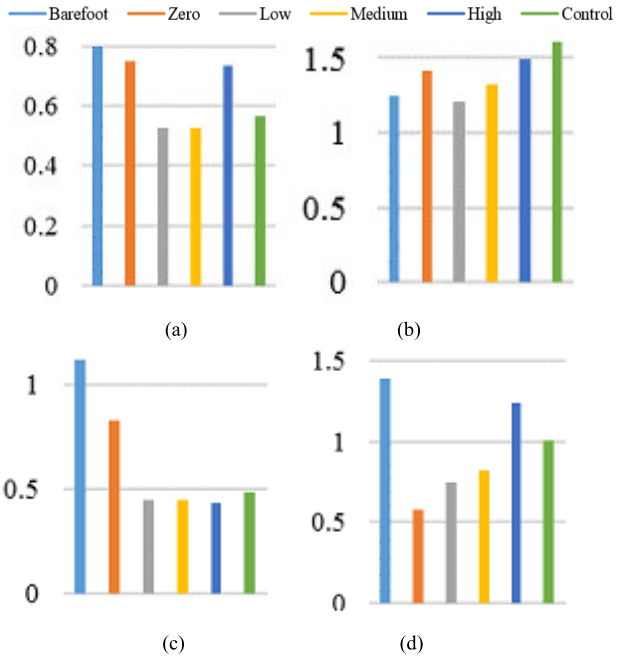

FIGURE 12. Average TA+G activity in different joint stiffness: (a) S1-WS1, (b) S1-WS2, (c) S2-WS1, (d) S2-WS2.

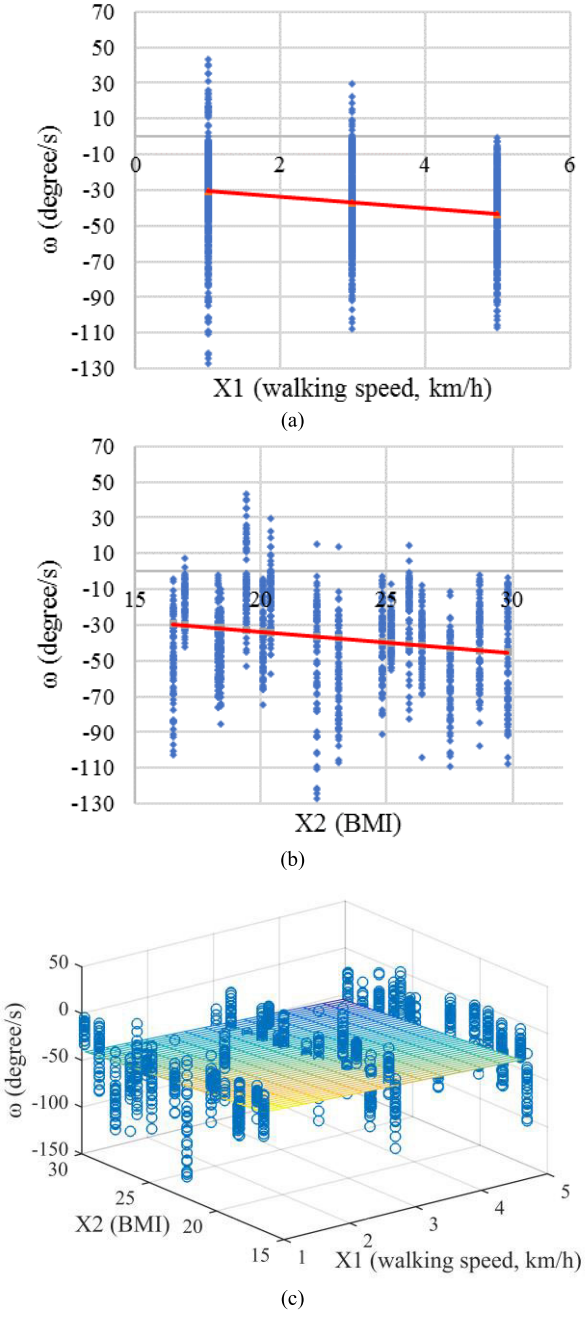

FIGURE 13. | Fig. 1. Regression analysis result of the ankle velocity in P1 with estimators: (a) X1 only, (b) X2 only, (c) Combination of X1 and X2. Blue dot is the actual ankle velocity data to build ω_{ref} function. Red line and yellow green blue plane is the estimated ankle velocity reference.

Theoretically, if the ankle joint is restricted, the TA should exert more force. However, the result shows a decrement instead of an increment. One possible explanation is that the subjects feel restricted when walking on the treadmill using the PICAFO. They let the treadmill move the leg backward during the stance (P2), resulting in ankle dorsiflexion without the TA muscle's need to work. Meanwhile, the G muscles maintain the forward force, where the PICAFO assistance naturally replaces the G muscle's work. Because of this, G activity was reduced significantly.

Meanwhile, the TA and G activities generally increase from P3 until the middle of P4. The push-off and toe clearance happen during this period. During P3, the G muscle generates a plantarflexion to push the foot off the ground so the body forward propulsion can happen. During the initial swing or P4, the TA dorsiflexes the foot to ensure toe clearance for

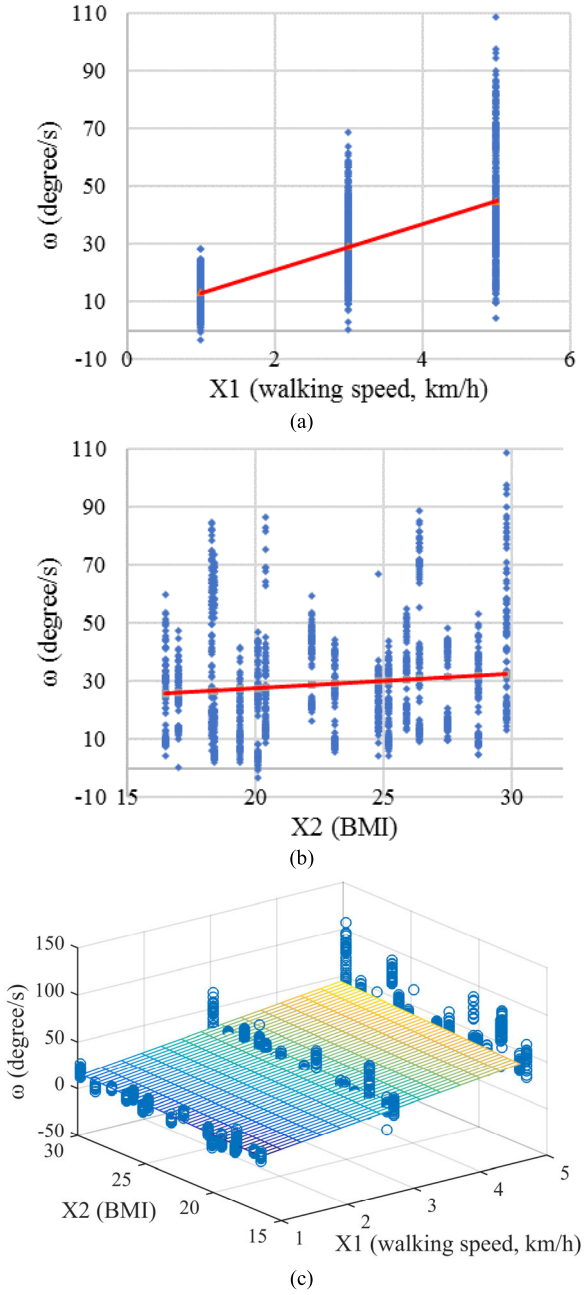

FIGURE 14. | **Fig. 2. Regression analysis result of the ankle velocity in P2 with estimators: (a) X1 only, (b) X2 only, (c) Combination of X1 and X2. Blue dot is the ankle velocity data to build ω_{ref} function. Red line and yellow green blue plane is the estimated ankle velocity reference.**

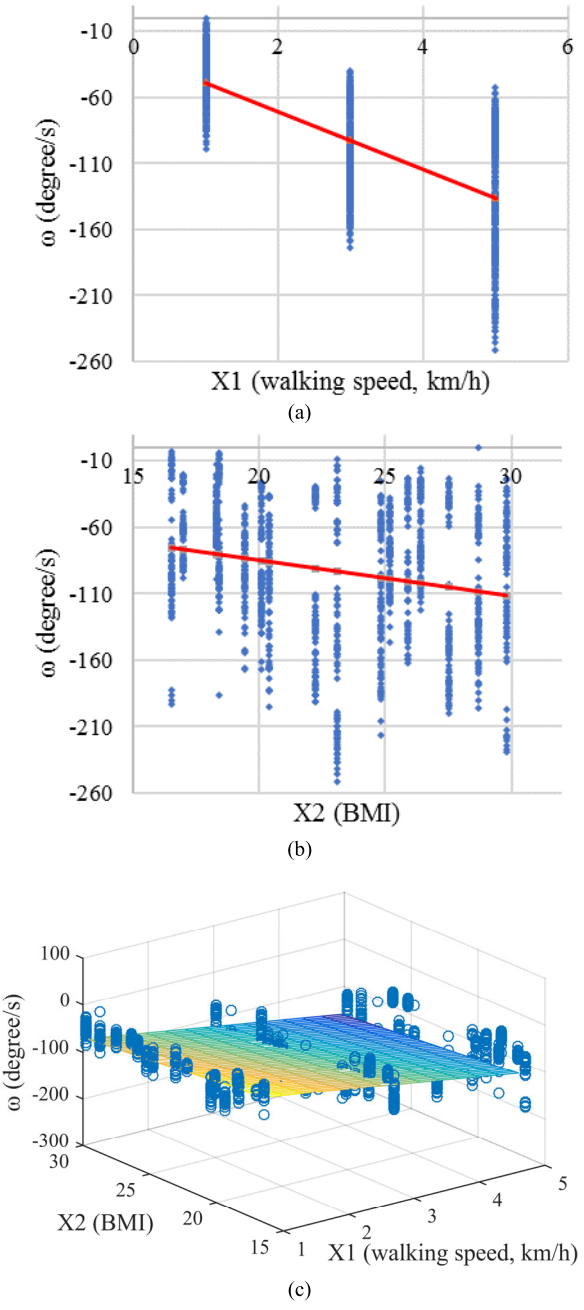

FIGURE 15. | **Fig. 3. Regression analysis result of the ankle velocity in P3 with estimators: (a) X1 only, (b) X2 only, (c) Combination of X1 and X2. Blue dot is the ankle velocity data to build ω ref function. Red line and yellow green blue plane is the estimated ankle velocity reference.**

the next walking step. These movements require minimum restriction; thus, the additional restriction will increase the muscle activity to perform the same movement. For example, the high stiffness resulted in the highest TA activity, as shown in cases involving S1-WS1 in Fig. 9. However, after achieving toe clearance, the TA needs to hold the foot position only. The need aligns with PICAFO's stiffness restriction. Thus, the TA activity was reduced during the middle to late swing or P4 due to PICAFO's stiffness restriction.

The PICAFO restricts the ankle movement, especially when stiffness is applied. The restriction affects the TA and G activity augmentation or reduction, as shown in Fig. 9. At some point, the TA activity may decrease, but at the same time, the G activity may increase due to the PICAFO ankle joint stiffness. A suitable amount of stiffness can minimize this kind of drawback by compromising the augmentation and reduction of TA and G muscle activity. However, a suitable amount of stiffness is different from person to person due to anthropometric differences, such as BMI or different walking speed preferences. Therefore, the ω_{ref} function developed in this study is essential, which enables PICAFO to control the walking gait with suitable joint stiffness.

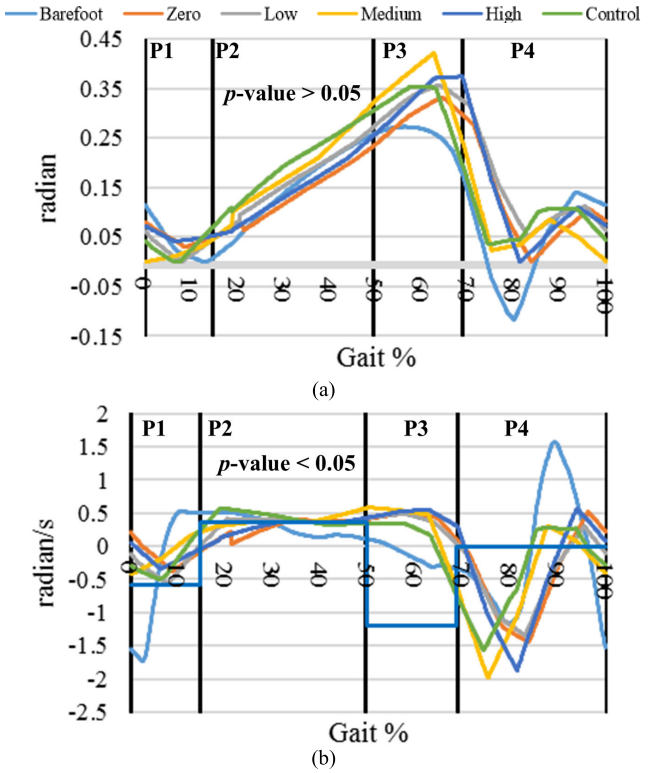

FIGURE 16. | **Fig. 1. Average ankle kinematics in different joint stiffness for case S1-WS2: (a) ankle position; (b) ankle velocity (ω_{ref} shown in solid straight line).**

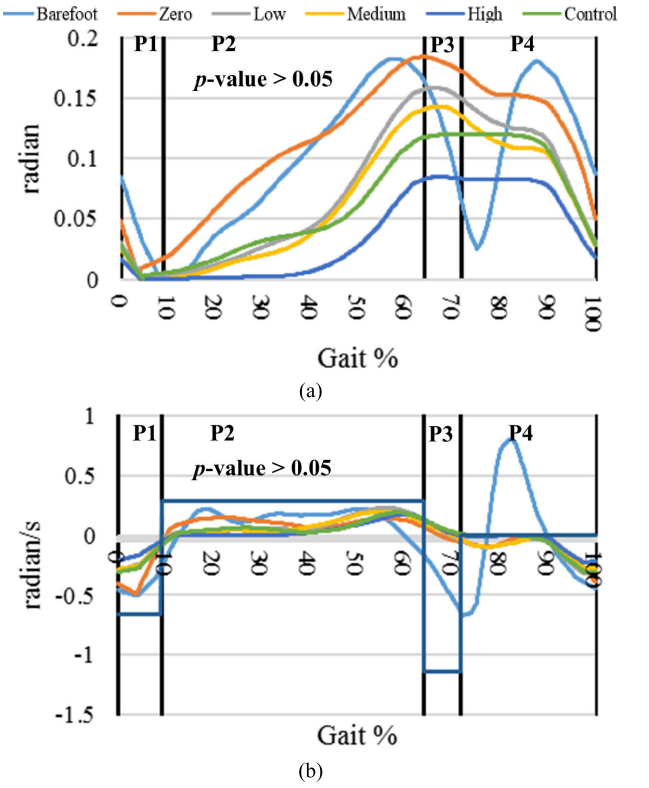

FIGURE 17. | **Fig. 2. Average ankle kinematics in different joint stiffness for case S2-WS1: (a) ankle position; (b) ankle velocity (ω_{ref} shown in solid straight line).**

The average muscle activity provides an understanding of joint stiffness that compromises muscle activity augmentation and reduction. Fig. 10 and Table 5 show the effect of different ankle joint stiffness on the average muscle activity of both S1 and S2 at different walking speeds (WS1 and WS2). The percentage number in Table 5 is calculated by comparing the muscle activity of PICAFO aided walking with muscle activity of walking barefooted. For instance, controlled stiffness in the S1-WS1 case resulted in overall muscle activity reduction by 29% compared to walking barefooted in the S1-WS1 case.

Refer to Table 5, S1 favors PICAFO with medium stiffness to reduce the TA activity by ∼39% and low stiffness to reduce the G activity by ∼32% in WS 1. The combined results of both muscle activities indicate that the medium stiffness PICAFO is the most suitable ankle stiffness for S1 in the case of WS1 compared to the low and high stiffness, which reduces the overall muscle activity by ∼34%. In the same WS1 case, the S2 favors different ankle joint stiffness, such as low stiffness to reduce the TA activity by ∼67%, high stiffness to reduce G activity by ∼58%, and high stiffness to compensate for both muscle activity reduction by ∼62%. In the case of WS2, both subjects also exhibit different muscle activity results. Low stiffness is more suitable for S1 compared to other forms of stiffness (muscle activity reduction of ∼3%), while zero stiffness is suitable for S2 (muscle activity reduction of ∼58%). These results prove that different walking speed people require unique ankle joint stiffness that needs to be supported by the PICAFO system.

Fig. 10, Fig. 11, and Fig. 12 also illustrate the effect of applying controlled stiffness to TA activity, G activity, and both muscle activities, respectively. The graph shows the average muscle activity, which is normalized to the highest barefooted muscle activity in that case. There are four graphs in each Fig. 10, Fig. 11, and Fig. 12, such as S1-WS1 (a), S1-WS2 (b), S2-WS1 (c), and S2-WS2 (d).

If the most suitable PICAFO stiffness is responsible for significantly reducing muscle activity, then the developed control stiffness will never be the most suitable PICAFO stiffness for both subjects. Except for the S1-WS2 case, the TA activity has resulted in the most muscle activity reduction by ∼25% when the controlled stiffness is applied. Despite that, the controlled stiffness is not the all-loser compared to the other ankle stiffness. For instance, the controlled stiffness is better (overall muscle activity reduced by ∼29%) than the high stiffness (overall muscle activity reduced by ∼8%) in the case of S1-WS1. Therefore, the use of the estimated ω_{ref} can decrease the trial and error process of prescribing a suitable ankle joint stiffness. Suppose the overall muscle activity can be further reduced compared to walking barefooted or with zero stiffness, as shown in the case of WS1 for both subjects. In that case, that stiffness is assumed to give positive assistance, which is achieved using the estimated ω_{ref} as the control reference.

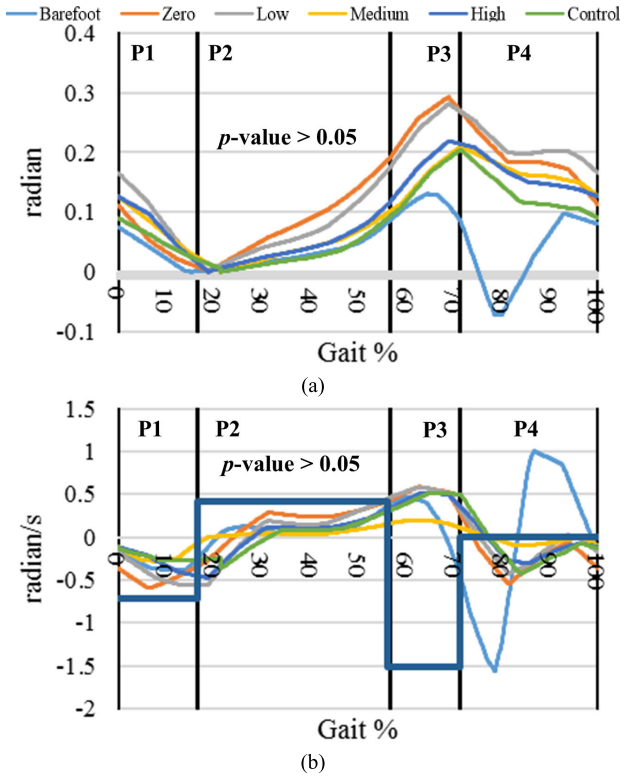

FIGURE 18. | **Fig. 3. Average ankle kinematics in different joint stiffness for case S2-WS2: (a) ankle position; (b) ankle velocity (ω_{ref} shown in solid straight line).**

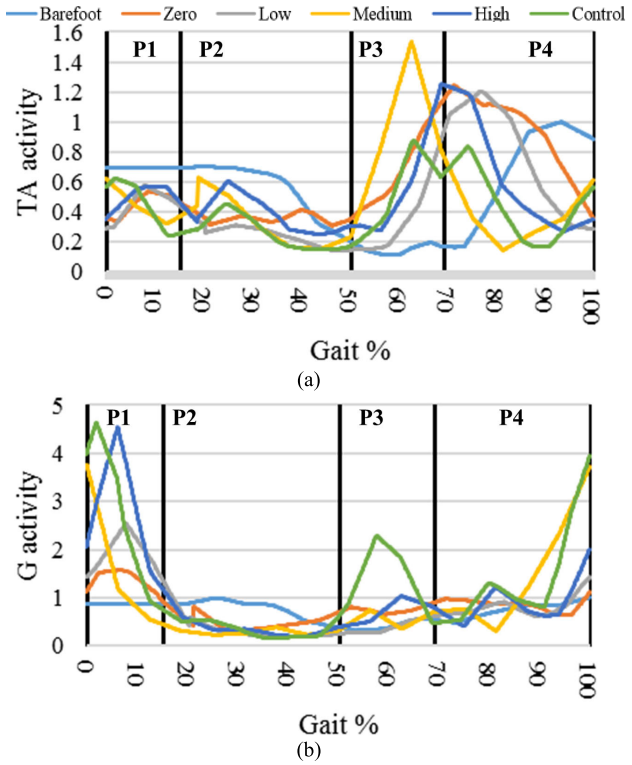

FIGURE 19. | **Fig. 1. RMS EMG of muscle activity in different joint stiffness for case S1-WS2: (a) Tibialis Anterior activity; (b) Gastrocnemius activity.**

However, the result of overall muscle activity reduction (TA+G) from PICAFO stiffness does not appear in both S1-WS2 and S2-WS2 cases. Although the TA activity reduces, the G activity does not decrease. This study's participating subject is the able-bodied subject who can do push-off, which requires plantarflexion with less restriction. Naturally, the push-off will get faster following the increase in the walking speed. More muscle force is required to achieve a higher speed, push-off under the restriction of PICAFO stiffness. Since the G is the muscle responsible for plantarflexion, it explains the high G activity in S1-WS2 and S2-WS2 case, as shown in Fig. 11.

The PICAFO controllers have initiated the foot push-off during P3 by having high plantarflexion ω_{ref}. In case of inaccurate detection, for example, when the PICAFO detects P4 instead of P3, the controller will instruct the MR brake to generate stiffness since it should lock the ankle position during P4. As a result, the muscle activity increases when performing the push-off. Meanwhile, if the PICAFO detects the gait correctly, then the MR brake will generate stiffness to sufficiently control the ω. Walking gait control using PICAFO allows muscle activity reduction. For example, TA activity reduction on P4 and G activity reduction on P2 are observed in Fig. 9.

The conventional rigid AFO by Delafontaine *et al.* [46] was reported to reduce TA activity. The unpowered AFO with spring [8] and the unpowered AFO with oil-damper [14] were reported to reduce G activity, especially on P2. However, PICAFO control stiffness reduced both TA and G activity by applying sufficient damping stiffness whenever necessary, based on the ω_{ref}. The TA was notably reduced in P1, P2, and the end of P4, unlike the results of the gait assistance using constant stiffness MR-Link by Hassan *et al.* [15] and Oba *et al.* [17] and soft actuator by Thalman *et al.* [47], where the TA reduced in P4 only. Even though the PICAFO only generates stiffness accordingly, the muscle activity reduction result is not inferior compared to the active powered AFO by Mazumder *et al.* [48]. S1 TA was reduced by ∼26%, and G was reduced by ∼31%, while Mazumder reported that the TA and G reductions were ∼26% and ∼29%, respectively. The comparison may not be fair because each work invites different subjects, uses various methods of controlling the ankle movement, and uses different test rigs or prototypes [49]. Therefore, further study should focus on increasing the subject numbers to evaluate the walking gait control performance using PICAFO with the improved estimated ω_{ref} based on walking speed and BMI.

V. CONCLUSION

This research has focused on improving passive AFO equipped with MR brake, called PICAFO by implementing ankle velocity as the control reference, based on walking speed and BMI. The control reference, which acts as the guidance of a control system, is crucial because it determines PICAFO's action to control the user's walking gait. A useful control reference should be able to adapt to different gait

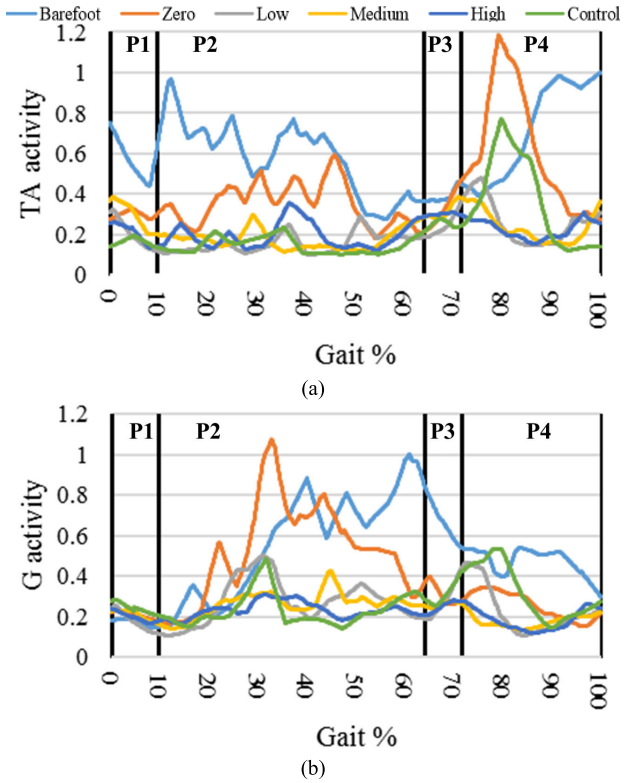

FIGURE 20. | **Fig. 2. RMS EMG of muscle activity in different joint stiffness for case S2-WS1: (a) Tibialis Anterior activity; (b) Gastrocnemius activity.**

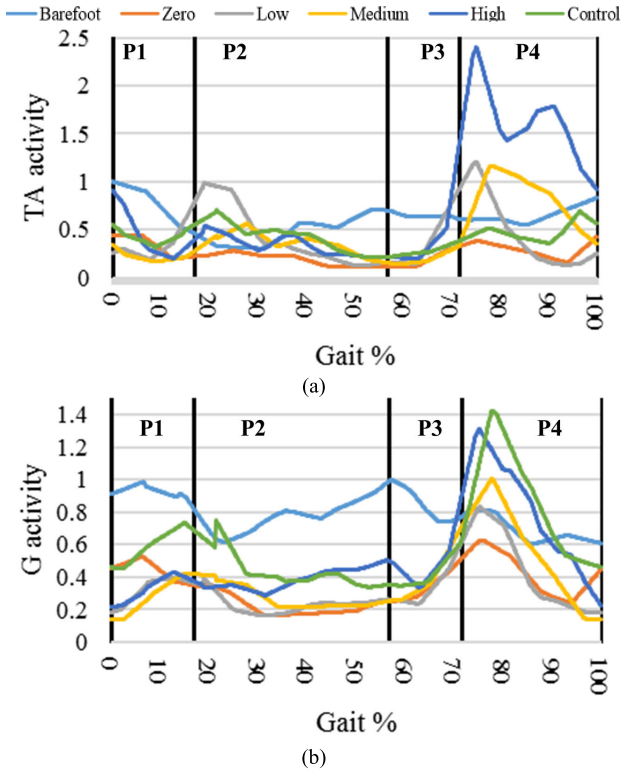

FIGURE 21. | **Fig. 3. RMS EMG of muscle activity in different joint stiffness for case S2-WS2: (a) Tibialis Anterior activity; (b) Gastrocnemius activity.**

phases, walking modes, and even subjects while at the same time not producing bulky devices due to over-specified actuators and sensors. Therefore, this study chooses the ankle velocity as the control reference (ω_{ref}) because it can be passively controlled using the MR brake and measured using a rotary encoder only (non-bulky sensor).

The investigation of ω_{ref} function shows that ω_{ref} for P1, P2, and P3 can be estimated based on walking speed and BMI, where both the independent variable's coefficient is significantly not to be zero (p-value < 0.05). The implementation result shows a positive effect (i.e., more energy-efficient walking [3]) of PICAFO's controlled stiffness to the able-bodied subject, who does not need any assistance. Therefore, PICAFO is also expected to give positive aid to people in need, such as post-stroke patients with foot drop. Primarily ankle kinematics and muscle activity result in P4 show that PICAFO achieves the toe clearance by locking the foot position (ankle velocity equals zero rad/s). Thus, it reduces muscle activity because the MR brake partially replaces the muscle work. This function is necessary for a post-stroke patient with foot drop who cannot lock the foot position by himself. Also, the controlled stiffness on P1, P2, and P3 makes the patient walks with less walking energy, as suggested by muscle activity reduction on P2.

This study's results serve as the groundwork for further developing a sophisticated PICAFO system, which can be adaptable to different gait phases, walking modes and can also be subjected to intensive and autonomous gait rehabilitation. Using the controlled stiffness, which is based on ω_{ref}, the therapist or doctor can do intensive, collaborative, and personalized AFO prescription [50]. They can skip the trial and error process of finding an appropriate control reference using the ω_{ref} function based on walking speed and BMI. Future works and recommendations for the PICAFO system, such as improving the ankle velocity reference estimation by increasing the sample sizes and ankle velocity-based gait phase detection to optimize sensor numbers, are demanded. Meanwhile, functionality validation of PICAFO with controlled stiffness for assisting the post-stroke patient should also be carried out.

APPENDIX

APPENDIX A. REGRESSION ANALYSIS OF ANKLE VELOCITY DATA

See figure 13, 14 and 15.

APPENDIX B. ANKLE KINEMATIC RESULT

See figure 16, 17 and 18.

APPENDIX C. MUSCLE ACTIVITY RESULT

See figure 19, 20 and 21.

ACKNOWLEDGMENT

The authors would like to express their gratitude to Universitas Sebelas Maret for supporting some of the hardware and the APC through Hibah Kolaborasi Internasional 2020 and the Institut Teknologi Telkom Surabaya for their partial support on APC.

REFERENCES

[1] R. Jiménez-Fabián and O. Verlinden, "Review of control algorithms for robotic ankle systems in lower-limb orthoses, prostheses, and exoskeletons," *Med. Eng. Phys.*, vol. 34, no. 4, pp. 397–408, May 2012.

[2] G. S. Sawicki and D. P. Ferris, "A pneumatically powered knee-ankle-foot orthosis (KAFO) with myoelectric activation and inhibition," *J. Neuroeng. Rehabil.*, vol. 6, no. 1, pp. 1–16, Dec. 2009.

[3] C. Liang and T. Hsiao, "Admittance control of powered exoskeletons based on joint torque estimation," *IEEE Access*, vol. 8, pp. 94404–94414, 2020.

[4] A. R. Emmens, E. H. F. van Asseldonk, and H. van der Kooij, "Effects of a powered ankle-foot orthosis on perturbed standing balance," *J. Neuroeng. Rehabil.*, vol. 15, no. 1, pp. 1–13, Dec. 2018.

[5] E. S. Schrank, L. Hitch, K. Wallace, R. Moore, and S. J. Stanhope, "Assessment of a virtual functional prototyping process for the rapid manufacture of passive-dynamic ankle-foot orthoses," *J. Biomech. Eng.*, vol. 135, no. 10, Oct. 2013, Art. no. 101011.

[6] J. A. Blaya and H. Herr, "Adaptive control of a variable-impedance ankle-foot orthosis to assist drop-foot gait," *IEEE Trans. Neural Syst. Rehabil. Eng.*, vol. 12, no. 1, pp. 24–31, Mar. 2004.

[7] C. Fleischer and G. Hommel, "EMG-driven human model for orthosis control," in *Human Interaction With Machines*, G. Hommel and S. Huanye, Eds. Dordrecht, The Netherlands: Springer, 2006, doi: 10.1007/1-4020-4043-1_8.

[8] S. H. Collins, M. B. Wiggin, and G. S. Sawicki, "Reducing the energy cost of human walking using an unpowered exoskeleton," *Nature*, vol. 522, no. 7555, pp. 212–215, Jun. 2015.

[9] A. W. Boehler, K. W. Hollander, T. G. Sugar, and D. Shin, "Design, implementation and test results of a robust control method for a powered ankle foot orthosis (AFO)," in *Proc. IEEE Int. Conf. Robot. Autom.*, May 2008, pp. 2025–2030.

[10] T. Kikuchi, S. Tanida, T. Yasuda, and T. Fujikawa, "Automatic adjustment of initial drop speed of foot for intelligently controllable ankle foot orthosis," in *Proc. IEEE/SICE Int. Symp. Syst. Integr.*, Dec. 2013, pp. 276–281.

[11] H. Naito, Y. Akazawa, K. Tagaya, T. Matsumoto, and M. Tanaka, "An ankle-foot orthosis with a variable-resistance ankle joint using a magnetorheological-fluid rotary damper," *J. Biomech. Sci. Eng.*, vol. 4, no. 2, pp. 182–191, 2009.

[12] D. van der Wilk, R. Reints, K. Postema, T. Gort, J. Harlaar, J. M. Hijmans, and G. J. Verkerke, "Development of an ankle-foot orthosis that provides support for flaccid paretic plantarflexor and dorsiflexor muscles," *IEEE Trans. Neural Syst. Rehabil. Eng.*, vol. 26, no. 5, pp. 1036–1045, May 2018.

[13] T. Kobayashi, "An articulated ankle–foot orthosis with adjustable plantarflexion resistance, dorsiflexion resistance and alignment: A pilot study on mechanical properties and effects on stroke hemiparetic gait," *Med. Eng. Phys.*, vol. 44, pp. 94–101, Jun. 2017.

[14] K. Ohata, T. Yasui, T. Tsuboyama, and N. Ichihashi, "Effects of an ankle-foot orthosis with oil damper on muscle activity in adults after stroke," *Gait Posture*, vol. 33, no. 1, pp. 102–107, Jan. 2011.

[15] M. Hassan, K. Yagi, H. Kadone, T. Ueno, H. Mochiyama, and K. Suzuki, "Optimized design of a variable viscosity link for robotic AFO," in *Proc. 41st Annu. Int. Conf. IEEE Eng. Med. Biol. Soc. (EMBC)*, Jul. 2019, pp. 6220–6223.

[16] D. Adiputra, M. A. A. Rahman, Ubaidillah, D. D. D. P. Tjahjana, P. J. Widodo, and F. Imaduddin, "Controller development of a passive control ankle foot orthosis," in *Proc. Int. Conf. Robot., Autom. Sci. (ICORAS)*, Nov. 2017, pp. 3–7.

[17] T. Oba, H. Kadone, M. Hassan, and K. Suzuki, "Robotic Ankle–Foot orthosis with a variable viscosity link using MR fluid," *IEEE/ASME Trans. Mechatronics*, vol. 24, no. 2, pp. 495–504, Apr. 2019.

[18] T. Kikuchi, S. Tanida, T. Yasuda, and T. Fujikawa, "Development of control model for intelligently controllable ankle-foot orthosis," in *Proc. 35th Annu. Int. Conf. IEEE Eng. Med. Biol. Soc. (EMBC)*, Jul. 2013, pp. 330–333.

[19] D. Adiputra, Ubaidillah, S. Mazlan, H. Zamzuri, and M. A. Rahman, "Fuzzy logic control for ankle foot equipped with magnetorheological brake," *J. Teknol.*, vol. 11, no. 11, pp. 25–32, 2016.

[20] D. Adiputra, N. Nazmi, I. Bahiuddin, U. Ubaidillah, F. Imaduddin, M. Abdul Rahman, S. Mazlan, and H. Zamzuri, "A review on the control of the mechanical properties of ankle foot orthosis for gait assistance," *Actuators*, vol. 8, no. 1, p. 10, Jan. 2019.

[21] P. P. Pott, S. I. Wolf, J. Block, S. van Drongelen, M. Grün, D. W. Heitzmann, J. Hielscher, A. Horn, R. Müller, O. Rettig, U. Konigorski, R. Werthschützky, H. F. Schlaak, and T. Meiß, "Knee-ankle-foot orthosis with powered knee for support in the elderly," *Proc. Inst. Mech. Eng., H, J. Eng. Med.*, vol. 231, no. 8, pp. 715–727, Aug. 2017.

[22] D. Adiputra, M. A. Abdul Rahman, Ubaidillah, S. A. Mazlan, N. Nazmi, M. K. Shabdin, J. Kobayashi, and M. H. Mohammed Ariff, "Control reference parameter for stance assistance using a passive controlled ankle foot Orthosis—A preliminary study," *Appl. Sci.*, vol. 9, no. 20, p. 4416, Oct. 2019.

[23] J. Furusho, "Development of shear type compact MR brake for the intelligent Ankle-Foot orthosis and its control; Research and development in NEDO for practical application of human support robot," in *Proc. IEEE 10th Int. Conf. Rehabil. Robot.*, Jun. 2007, pp. 89–94.

[24] U. F. Imaduddin, M. Nizam, and S. A. Mazlan, "Response of a magnetorheological brake under inertial loads," *Int. J. Elect. Eng. Inform.*, vol. 7, no. 2, pp. 308–322, 2015.

[25] F. H. Hidayatullah, Ubaidillah, E. D. Purnomo, D. D. D. P. Tjahjana, and I. B. Wiranto, "Design and simulation of a combined serpentine T-shape magnetorheological brake," *Indonesian J. Elect. Eng. Comput. Sci.*, vol. 13, no. 3, pp. 1221–1227, 2019.

[26] V. M. Capture. (2016). *Plug-in Gait Reference Guide*. [Online]. Available: https://docs.vicon.com/download/attachments/50888706/Plug-in Gait Reference Guide.pdf?version=1&modificationDate=1512999736000&api=v2

[27] T. Kikuchi, S. Tanida, K. Otsuki, T. Yasuda, and J. Furusho, "Development of third-generation intelligently controllable ankle-foot orthosis with compact MR fluid brake," in *Proc. IEEE Int. Conf. Robot. Autom.*, May 2010, pp. 2209–2214.

[28] T. Kikuchi, S. Tanida, K. Otsuki, T. Kakehashi, J. Furusho, "Development of intelligent ankle-foot orthosis (i-AFO) with MR fluid brake and control system for gait control," in *Service Robotics and Mechatronics*, K. Shirase and S. Aoyagi, Eds. London, U.K.: Springer, 2010, doi: 10.1007/978-1-84882-694-6_13.

[29] S. Tanida, T. Kikuchi, T. Kakehashi, K. Otsuki, T. Ozawa, T. Fujikawa, T. Yasuda, J. Furusho, S. Morimoto, and Y. Hashimoto, "Intelligently controllable ankle foot orthosis (I-AFO) and its application for a patient of guillain-barre syndrome," in *Proc. IEEE Int. Conf. Rehabil. Robot.*, Jun. 2009, pp. 857–862.

[30] D. A. Winter, *Biomechanics and Motor Control of Human Movement*, 2nd ed. Hoboken, NJ, USA: Wiley, 2009, doi: 10.1002/9780470549148.

[31] S. V. Gill, "The impact of weight classification on safety: Timing steps to adapt to external constraints," *J. Musculoskelet. Neuronal Interact.*, vol. 15, no. 1, pp. 103–108, 2015.

[32] B. Chen, X. Zhao, H. Ma, L. Qin, and W.-H. Liao, "Design and characterization of a magneto-rheological series elastic actuator for a lower extremity exoskeleton," *Smart Mater. Struct.*, vol. 26, no. 10, 2017, Art. no. 105008.

[33] A. Moraux, A. Canal, G. Ollivier, I. Ledoux, V. Doppler, C. Payan, and J.-Y. Hogrel, "Ankle dorsi- and plantar-flexion torques measured by dynamometry in healthy subjects from 5 to 80 years," *BMC Musculoskeletal Disorders*, vol. 14, no. 1, Dec. 2013.

[34] K. Godziuk, C. M. Prado, L. J. Woodhouse, and M. Forhan, "Prevalence of sarcopenic obesity in adults with end-stage knee osteoarthritis," *Osteoarthritis Cartilage*, vol. 27, no. 12, pp. 1735–1745, Dec. 2019.

[35] L.-F. Yeung, C. Ockenfeld, M.-K. Pang, H.-W. Wai, O.-Y. Soo, S.-W. Li, and K.-Y. Tong, "Randomized controlled trial of robot-assisted gait training with dorsiflexion assistance on chronic stroke patients wearing ankle-foot-orthosis," *J. Neuroeng. Rehabil.*, vol. 15, no. 1, pp. 1–12, Dec. 2018.

[36] S. F. Tyson, A. Vail, N. Thomas, K. Woodward-Nutt, S. Plant, and P. J. Tyrrell, "Bespoke versus off-the-shelf ankle-foot orthosis for people with stroke: Randomized controlled trial," *Clin. Rehabil.*, vol. 32, no. 3, pp. 367–376, Mar. 2018.

[37] A. K. Mishra, A. Srivastava, R. P. Tewari, and R. Mathur, "EMG analysis of lower limb muscles for developing robotic exoskeleton orthotic device," *Procedia Eng.*, vol. 41, pp. 32–36, 2012.

[38] N. Nazmi, "Assessment on stationarity of EMG signals with different windows size during isotonic contractions," *Appl. Sci.*, vol. 7, no. 10, p. 1050, 2017.

[39] N. Nazmi, M. A. Abdul Rahman, S.-I. Yamamoto, and S. A. Ahmad, "Walking gait event detection based on electromyography signals using artificial neural network," *Biomed. Signal Process. Control*, vol. 47, pp. 334–343, Jan. 2019.

[40] B. Rodríguez-Tapia, I. Soto, D. M. Marínez, and N. C. Arballo, "Myoelectric interfaces and related applications: Current state of EMG signal processing—A systematic review," *IEEE Access*, vol. 8, pp. 7792–7805, 2020.
[41] F. B. Rodrigues, A. O. Andrade, and M. F. Vieira, "Effects of inclined surfaces on gait variability and stability in unilateral lower limb amputees," *Med. Biol. Eng. Comput.*, vol. 57, no. 11, pp. 2337–2346, Nov. 2019.
[42] M. Moltedo, T. Bačekk, T. Verstraten, C. Rodriguez-Guerrero, B. Vanderborght, and D. Lefeber, "Powered ankle-foot orthoses: The effects of the assistance on healthy and impaired users while walking," *J. Neuroeng. Rehabil.*, vol. 15, no. 1, p. 86, Dec. 2018.
[43] K. E. Gordon and D. P. Ferris, "Learning to walk with a robotic ankle exoskeleton," *J. Biomech.*, vol. 40, no. 12, pp. 2636–2644, Jan. 2007.
[44] J. A. Blaya and H. Herr, "Adaptive control of a variable-impedance ankle-foot orthosis to assist drop-foot gait," *IEEE Trans. Neural Syst. Rehabil. Eng.*, vol. 12, no. 1, pp. 24–31, Mar. 2004, doi: 10.1109/TNSRE.2003.823266.
[45] A. Daryabor, M. Arazpour, and G. Aminian, "Effect of different designs of ankle-foot orthoses on gait in patients with stroke: A systematic review," *Gait Posture*, vol. 62, pp. 268–279, May 2018.
[46] A. Delafontaine, O. Gagey, S. Colnaghi, M.-C. Do, and J.-L. Honeine, "Rigid ankle foot orthosis deteriorates mediolateral balance control and vertical braking during gait initiation," *Frontiers Human Neurosci.*, vol. 11, pp. 1–10, Apr. 2017.
[47] C. M. Thalman, J. Hsu, L. Snyder, and P. Polygerinos, "Design of a soft ankle-foot orthosis exosuit for foot drop assistance," in *Proc. Int. Conf. Robot. Autom. (ICRA)*, May 2019, pp. 8436–8442.
[48] O. Mazumder, A. Kundu, P. Lenka, and S. Bhaumik, "Robotic AFO to enhance walking capacity: Initial development," *Electron. Lett.*, vol. 52, no. 22, pp. 1840–1841, Oct. 2016.
[49] D. Totah, M. Menon, C. Jones-Hershinow, K. Barton, and D. H. Gates, "The impact of ankle-foot orthosis stiffness on gait: A systematic literature review," *Gait Posture*, vol. 69, pp. 101–111, Mar. 2019.
[50] K. Kane, P. Manns, J. Lanovaz, and K. Musselman, "Clinician perspectives and experiences in the prescription of ankle-foot orthoses for children with cerebral palsy," *Physiotherapy Theory Pract.*, vol. 35, no. 2, pp. 148–156, Feb. 2019.

DIMAS ADIPUTRA was born in Jakarta, Indonesia, in 1993. He received the Ph.D. degree in medical instrumentation from Universiti Teknologi Malaysia, Malaysia, in 2020. He is currently an Assistant Professor with the Electrical Engineering Department, Institut Teknologi Telkom Surabaya, Indonesia. His research interests include health care devices and the Internet of Things, where the ultimate goal is health care services or facilities that transcend the distance for everyone.

MOHD AZIZI ABDUL RAHMAN (Senior Member, IEEE) received the Ph.D. degree from the Shibaura Institute of Technology, Japan. He is currently a Senior Lecturer with the Malaysia-Japan International Institute of Technology, Universiti Teknologi Malaysia. His primary research interests include bio signal processing and control towards robotics devices development like exoskeleton and orthosis. He has published his research works at several international journals, conference proceedings, and books.

UBAIDILLAH (Senior Member, IEEE) received the master's degree in semi-active automotive suspension system using magnetorheological (MR) dampers from Universiti Teknikal Malaysia (UteM), Melaka, Malaysia, in 2010, and the Ph.D. degree from the Malaysia-Japan International Institute of Technology, Universiti Teknologi Malaysia, in 2016. He is currently an Associate Professor of Mechanical Engineering with the Faculty of Engineering, Universitas Sebelas Maret, Indonesia. He has been studying MR technologies, since 2007, starting from development of device-based MR, such as MR damper, MR brake, MR clutch, and MR engine mounting. He began a research on MR materials, since 2012, which focused on MR elastomers, MR grease, MR foam, and MR fluids. He has managed to publish about 75 indexed articles in MR fields.

SAIFUL AMRI MAZLAN received the Ph.D. degree from Dublin City University, Ireland. He is currently a Professor with the Malaysia-Japan International Institute of Technology, Universiti Teknologi Malaysia. He is a registered Professional Engineer with the Board of Engineers Malaysia. His research interest includes magnetorheological (MR) materials, where these materials undergo significant responses leading to consequent rheological changes upon the influence of magnetic field. The materials can offer tremendous opportunities for variable stiffness devices. He has published his research works at several international journals and conference proceedings.